Progress In Electromagnetics Research, PIER 78, 49–59, 2008

MODELING WITH NURBS SURFACES USED FOR THE CALCULATION OF RCS

Y. Zhao, X.-W. Shi, and L. Xu

National Key Lab of Antennas and Microwave Technology
Xidian University
Xi'an, 710071, China

Abstract—In this paper, the edge-facet model is transformed to the Non-Uniform Rational B-Spline (NURBS) model. The parameters of the knot vectors and the control points of NURBS are computed based on the data points on the surface of a target, and the NURBS model is constructed with the parameters. The degrees of the two parametric directions of a NURBS surface and the B-spline basis function are also analyzed. The relative errors between the NURBS models and the real models prove that the modeling method proposed in this paper is exact. Finally, the results of the Radar Cross Section (RCS) computed by the Physical Optics (PO) method with NURBS models are illustrated, and the results prove that the modeling method is of high precision and can be widely used in computational electromagnetics techniques.

1. INTRODUCTION

The technology of electromagnetic modeling is one of the hottest issues in Computational Electromagnetics, and it is one of the most important problems in the RCS calculation [1–10].

Although the edge-facet model [11] built from elements of flat patches gives a great improvement over other geometrical descriptions, a large number of facets is needed to fit curved surfaces. With the development of Computer Aided Geometric Design (CAGD), NURBS [5–10] technique is currently widely used in many industries to represent complex bodies. The method is quite efficient because it makes use of a small number of patches to model complex bodies, so it requires very little memory and computing time. For instance, a spherical surface can be modeled perfectly with only one NURBS surface, but hundreds of triangle facets are needed to model a spherical surface (see Fig. 1); a complex body, such as a complete aircraft, can

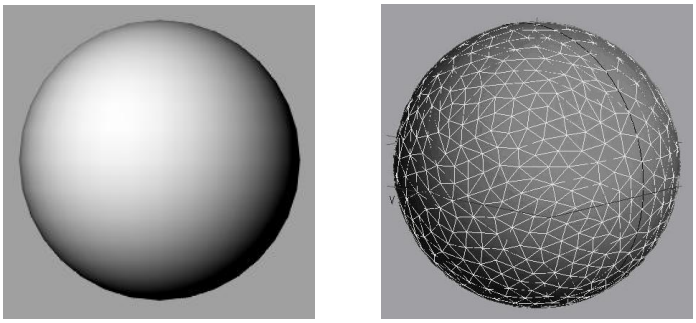

(a) (b)

Figure 1. A spherical surface using (a) a NURBS surface (b) triangle facets.

be described with nearly all its details, and a precision of 1mm, by only a few hundred NURBS patches [7].

In Computational Electromagnetics, many scholars do their best to study the methods for computing RCS with NURBS surface models. There have been many methods which are used with NURBS models for calculating RCS, such as the Moment Method (MOM) [5, 6], the Physical Optics (PO) method [6–10], the Geometrical Optics (GO) method [9], the Equivalent Currents Method (EMC) [9, 10], and so on. But the most models which have existed are edge-facet models, and to a real model it is impossible to obtain NURBS parameters directly. So it is necessary to transform the existent model to the model which is modeled with NURBS surfaces.

In this paper, objects are modeled with NURBS surfaces by calculating the parameters of the knot vectors and the control points of NURBS. The degrees of the two parametric directions of a NURBS surface and the B-Spline basis function are also analyzed. Then the RCS of objects modeled with NURBS surfaces is computed by PO, and the key integral is calculated with Ludwig's integral method.

2. THEORY

2.1. Calculating the RCS with PO Method

The RCS is defined as [7, 10, 12]:

$$\sigma = \lim_{R\to\infty} 4\pi R^2 \frac{\left|\vec{E}^s\right|^2}{\left|\vec{E}^i\right|^2} \tag{1}$$

To perfect conductor, if the RCS is computed by PO, the backscattering electric field will be:

$$\vec{E}^s = \frac{2k^2 e^{jkr}}{j\omega\varepsilon 4\pi r} \cdot \int_{s'} e^{-jk\hat{r}\cdot\vec{r}'} \left\{ \hat{r} \left[\hat{r} \cdot \left(\hat{n} \times \vec{H}^i \right) \right] - \left[\hat{n} \times \vec{H}^i \right] \right\} ds' \tag{2}$$

If plane wave is given, then

$$\vec{E}^i = \vec{E}^0 e^{j\vec{k}\cdot\vec{r}'}, \qquad \vec{H}^i = \hat{k} \times \vec{E}^i \tag{3}$$

So, the formula (2) can be rewritten as:

$$\vec{E}^s = \frac{-je^{jkr}}{\lambda r} \vec{E}^0 \int_{s'} e^{2j\vec{k}\cdot\vec{r}'} (\hat{k} \cdot \hat{n}) ds' \tag{4}$$

Where

$$\hat{r} = -\hat{k} \tag{5}$$

Then, the RCS formula would be:

$$\sigma = \frac{4\pi}{\lambda^2} \left| \hat{k} \cdot \vec{I} \right|^2 \tag{6}$$

Where

$$\vec{I} = \int_{s'} \hat{n}(\vec{r}') e^{-j2k\hat{k}\cdot\vec{r}'} ds' \tag{7}$$

For NURBS patches

$$\hat{n} = \frac{\vec{r}_u \times \vec{r}_v}{|\vec{r}_u \times \vec{r}_v|} \tag{8}$$

$$ds' = |\vec{r}_u \times \vec{r}_v| \, dudv \tag{9}$$

Then, the formula (7) can also be expressed as:

$$\vec{I} = \int_{u=0}^{u=1} \int_{v=0}^{v=1} \vec{F}(u,v) e^{jk\gamma(u,v)} dudv \tag{10}$$

Where

$$\vec{F}(u,v) = \vec{r}_u(u,v) \times \vec{r}_v(u,v) \tag{11}$$

$$\gamma(u,v) = -2\hat{k} \cdot \vec{r}' \tag{12}$$

Formula (10) is the key integral for RCS computation.

Where, λ is the wavelength, $\hat{k}$ is the wave vector, s' is the body surface, r' is the surface point corresponding to ds', $\hat{n}$ is the unit normal vector at the point. The surface points $\vec{r}'(u,v)$ are given by the formula of the NURBS surface.

The formula (10) can be computed by Ludwig's integral method which was presented by Ludwig in 1968 [12].

2.2. Modeling with NURBS Surfaces

The NURBS surface is defined as [13]:

$$\vec{r}(u,v) = \frac{\sum_{i=0}^{m}\sum_{j=0}^{n} \omega_{i,j}\vec{d}_{i,j}N_{i,p}(u)N_{j,l}(v)}{\sum_{i=0}^{m}\sum_{j=0}^{n} \omega_{i,j}N_{i,p}(u)N_{j,l}(v)} \tag{13}$$

Where, $\vec{d}_{i,j}\,(i = 0, 1, \ldots, m;\ j = 0, 1, \ldots, n)$ are the control points. $\omega_{i,j}$ are the weights corresponding to $\vec{d}_{i,j}$. p and l are the degrees of the two parametric directions of a NURBS surface. $N_{i,p}(u)\,(i = 0, 1, \ldots, m)$ and $N_{j,l}(v)\,(j = 0, 1, \ldots, n)$ are canonical B-spline basis functions, and they are defined as the Cox-de-Boor formula with the knot vectors, $\vec{U} = [u_0, u_1, \ldots, u_{m+p+1}]$ and $\vec{V} = [v_0, v_1, \ldots, v_{n+l+1}]$, as follows [13]:

$$\begin{cases} N_{i,0} = \begin{cases} 1 & u_i \le u < u_{i+1} \\ 0 & \text{others} \end{cases} \quad \ldots\ldots\ldots\ldots\ldots\ldots\ldots\ldots\ldots\ldots..(a) \\ N_{i,p}(u) = \dfrac{u-u_i}{u_{i+p}-u_i}N_{i,p-1}(u) + \dfrac{u_{i+p+1}-u}{u_{i+p+1}-u_{i+1}}N_{i+1,p-1}(u)\ldots(b) \\ \text{if,} \quad \dfrac{0}{0} = 0 \ldots\ldots\ldots\ldots\ldots\ldots\ldots\ldots\ldots\ldots\ldots\ldots\ldots..(c) \end{cases} \tag{14}$$

2.2.1. Computing the Control Points of NURBS

Although to a real model, it is impossible to get the control points of NURBS directly, the data points on the surface of a target can be obtained easily. So, the control points should be calculated firstly by the data points $\vec{q}_{i,j}\,(i = 0, 1, \ldots, r;\ j = 0, 1, \ldots, s)$. Computing the control points of a NURBS surface needs transforming to computing the control points of a series of NURBS curves.

(12) can also be expressed as follows:

$$\vec{r}(u,v) = \frac{\sum_{i=0}^{m}\left(\sum_{j=0}^{n}\omega_{i,j}\vec{d}_{i,j}N_{j,l}(v)\right)N_{i,p}(u)}{R} = \frac{\sum_{i=0}^{m}\vec{d}_i(v)N_{i,p}(u)}{R} \tag{15}$$

Where

$$R = \sum_{i=0}^{m}\sum_{j=0}^{n}\omega_{i,j}N_{i,p}(u)N_{j,l}(v) \tag{16}$$

$$\vec{d}_i'(v) = \sum_{j=0}^{n} \omega_{i,j} \vec{d}_{i,j} N_{j,l}(v) \tag{17}$$

For

$$\vec{r}(u_i, v_j) = \vec{q}_{i-p,j-l} \, (i = p, p+1, \ldots, m+1; \; j = l, l+1, \ldots, n+1) \tag{18}$$

Where

$$u_i \in \vec{U}, \quad v_j \in \vec{V} \quad m = r + p - 1, \quad n = s + l - 1$$

Then the control points of (15), $\vec{d}_i'(v)$, can be calculated based on the data points $\vec{q}_{i,j} \, (i = 0, 1, \ldots, r; \; j = 0, 1, \ldots, s)$. Further, considering $\vec{d}_i'(v)$ as the data points, the control points of (16), $\vec{d}_{i,j} \, (i = 0, 1, \ldots, m; \; j = 0, 1, \ldots, n)$ which are also the control points of the NURBS surface, can be calculated [13].

2.2.2. The B-spline Basis Function

The canonical B-spline, which is defined as (13), is one of the most important techniques of NURBS.

In (13), u is the independent variable, and $0 \leq u < 1$. $\vec{U} = [u_0, u_1, \ldots, u_{m+p+1}]$ is a non-decreasing sequence of real numbers, i.e., $u_i \leq u_{i+1} \, (i = 0, 1, \ldots, m + p)$, and u_i is called a knot.

B-spline basis functions possess the following properties:
(i) The computation of a set of basis functions requires specification of the degree p and a knot vector $\vec{U}$.
(ii) $N_{i,p}(u) \geq 0$ for all i, p, and u (nonnegativity).
(iii) $\sum_i N_{i,p}(u) = 1$ for all $u \in [u_i, u_{i+1})$ (partition of unity).
(iv) $N_{i,0}(u)$ is a step function, equal to zero everywhere except on the half-open interval $u \in [u_i, u_{i+1})$. $N_{i,p}(u) = 0$ if u is outside of the interval $[u_i, u_{i+p+1})$ (local support property).

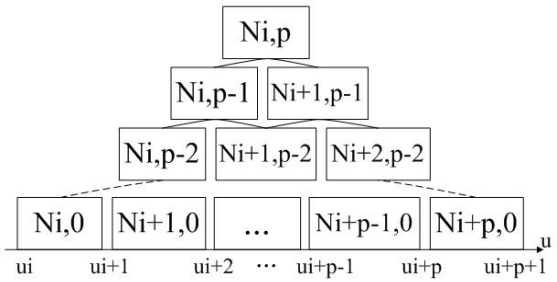

(v) If $u = 1$, all of the B-spline basis functions equal zero.
(vi) The length of the zero-degree B-spline basis function is $m + p + 1$. The length of the one-degree B-spline basis function is one less than that of the zero-degree B-spline basis function. Analogically, the length of the p-degree B-spline function is $m + 1$.
(vii) In any given knot span $[u_i, u_{i+1})$, at most $p + 1$ of the $N_{i,p}(u)$ are nonzero, namely the functions $N_{i-p,p}, \ldots, N_{i,p}$.

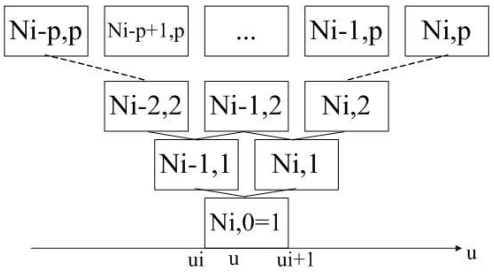

(viii) If $u_{i+p} = u_i$, then $u_i = u_{i+1} = \cdots = u_{i+p}$.

If $u > u_i$, $N_{i,0} = \cdots = N_{i+p-1,0} = 0$, then $N_{i,1} = \cdots = N_{i+p-2,1} = 0$, and analogically, $N_{i,p-1} = 0$.

If $u < u_i$, $N_{i,0} = \cdots = N_{m+p,0} = 0$, $N_{i,1} = \cdots = N_{m+p-1,1} = 0$, analogically, $N_{i,p-1} = \cdots = N_{m+1,p-1} = 0$.

So, when $u_{i+p} = u_i$, $N_{i,p-1} = 0$.

Similarly, when $u_{i+p+1} = u_{i+1}$ and $u \neq u_{i+p+1}$, $N_{i+1,p-1} = 0$.

2.2.3. The Degrees of the Two Parametric Directions

In this paper, the degrees (the degree k in the u direction and the degree l in the v direction) of a NURBS surface are considered by the way that a curve is modeled by the three-degree NURBS curve, and a beeline is modeled by the one-degree NURBS curve, which can reduce the computing amount and the computing time.

For example, a spherical surface is modeled with NURBS surface of 3×3 degrees, a cylindrical surface is modeled with NURBS surface of 3×1 degrees, and a plane is modeled with NURBS surface of 1×1 degrees.

2.2.4. Computing the Knot Vectors

The knot vectors of a NURBS surface, $\vec{U} = [u_0, u_1, \ldots, u_{m+p+1}]$ and $\vec{V} = [v_0, v_1, \ldots, v_{n+l+1}]$, can be computed as follows [13], with the canonical parameters of the data points $\vec{q}_{i,j}$, $(\tilde{u}_i, \tilde{v}_j)$, where $i =$

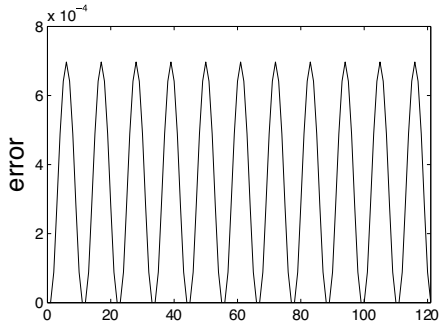

Figure 2. The relative errors of the radius of a cylindrical surface.

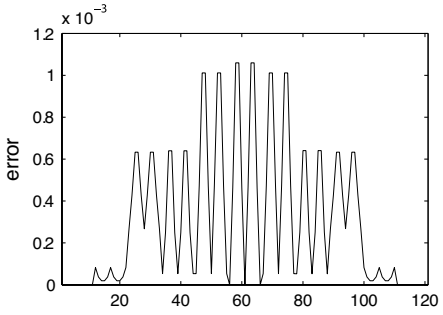

Figure 3. The relative errors of the radius of a spherical surface.

$0, \ldots, r;\ j = 0, \ldots, s.$

$$(u_i, v_j) = (\tilde{u}_{i-p}, \tilde{v}_{j-1}) \quad (i = p, p+1, \ldots, m+1;\ j = l, l+1, \ldots, n+1) \tag{19}$$

To the direction of u, if $\vec{q}_{0,j} \neq \vec{q}_{r,j}\,(j = 0, 1, \ldots, s)$, then

$$u_0 = u_1 = \cdots = u_p = 0, \quad u_{m+1} = u_{m+2} = \cdots = u_{m+p+1} = 1 \tag{20}$$

If $\vec{q}_{0,j} = \vec{q}_{r,j}\ (j = 0, 1, \ldots, s)$, then

$$\begin{aligned} u_0 &= u_{m-p+1} - 1, \quad u_1 = u_{m-p+2} - 1, \ldots, u_{p-1} = u_m - 1; \\ u_{m+2} &= 1 + u_{p+1}, \quad u_{m+3} = 1 + u_{p+2}, \ldots, u_{m+p+1} = 1 + u_{2p} \end{aligned} \tag{21}$$

Similarly, $v_0, \ldots, v_{l-1};\ v_{n+2}, \ldots, v_{n+l+1}$ can be calculated.

3. RESULTS AND DISCUSSION

Fig. 2 shows the relative errors of the radius of a cylindrical surface between the the NURBS model and the real model. And Fig. 3 shows the relative errors of the radius of a spherical surface.

As shown in Fig. 2 and Fig. 3, the relative errors between the NURBS model and the real model less than the order of 10^{-3}. And the errors can be accepted in Computational Electromagnetics.

Fig. 4 shows the real model of F16, and Fig. 5 shows the F16 modeled with NURBS surfaces. A missile whose length is nearly 1.6 m is depicted in Fig. 6, and a airplane is depicted in Fig. 7. In Fig. 6 and Fig. 7, the solid expressed the real models and the points denote the NURBS models. As shown in the figures, the NURBS models obtained by the modeling method mentioned in this paper match very well with the real models.

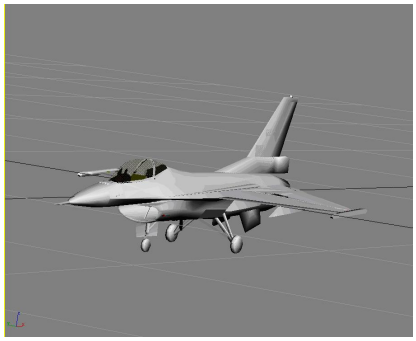

Figure 4. The real model of F16.

Figure 5. The NURBS model of F16.

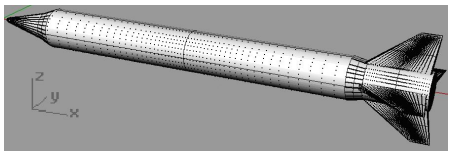

Figure 6. Representation of a missile.

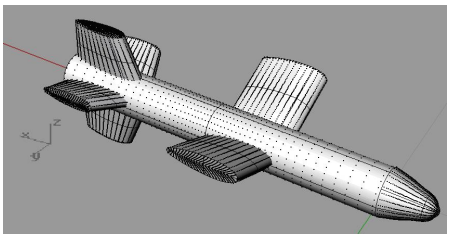

Figure 7. Representation of a airplane.

Fig. 8 shows the RCS of the cylinder above whose radius is 7 cm and height is 71.1 cm, with the frequency of 5.4 GHz. The result obtained by this paper is compared with the measurement in [14]. Fig. 9 presents the RCS of F16 which is shown in Fig. 5, with the frequency of 10 GHz, and the RCS of F16 computed in this paper is compared with the measurement in [15]. In the two figures, we can see, the results of the RCS obtained by PO method with NURBS models in this paper match very well with the measurements.

The RCS of the missile which is shown in Fig. 6 is presented in Fig. 10, and the frequency of the analysis is 2 GHz. The RCS of the airplane which is expressed in Fig. 7 is shown in Fig. 11, and the frequency is 3 GHz. The results are obtained for a cut with $\theta = 90°$ varying the incidence direction according to ϕ. As shown in the two figures, the results obtained in this paper, which are computed by PO method with NURBS models, match well with the results calculated by MOM with triangle-facet models and by PO with triangle-facet models.

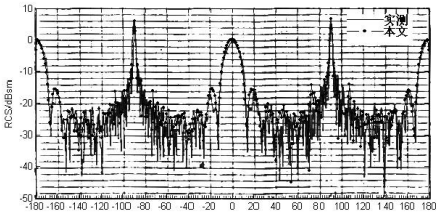

Figure 8. The RCS of the cylindrical above.

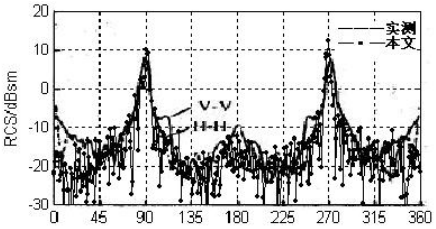

Figure 9. The RCS of F16 in Fig. 5.

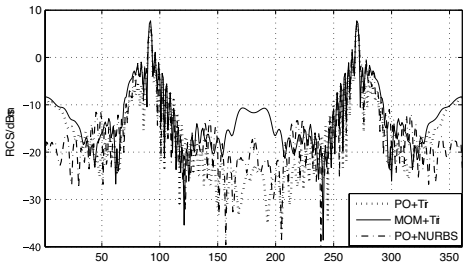

Figure 10. The RCS of the missile.

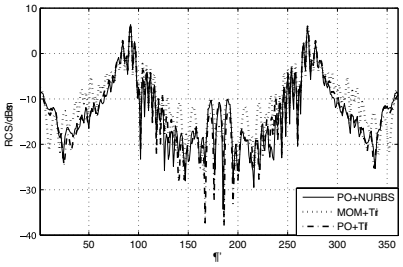

Figure 11. The RCS of the airplane.

4. CONCLUSION

In this paper, the edge-facet model is transformed to the NURBS model with a high precision, which can make the RCS calculation methods that are based on the NURBS model be used more widely. The results of the RCS, which are computed by PO method with NURBS models in this paper, match well with the measurements and the results calculated by other methods, and they verify the validity of the modeling method in Computational Electromagnetics.

REFERENCES

1. El-Ocla, H., "On laser radar cross section of targets with large sizes for E-polarization," *Progress In Electromagnetics Research*, PIER 56, 323–333, 2006.
2. Jin, K. S., T. I. Suh, S. H. Suk, B. C. Kim, and H. T. Kim, "Fast ray tracing using a space-division algorithm for rcs prediction," *Journal of Electromagnetic Waves and Applications*, Vol. 20, No. 1, 119–126, 2006.

3. Yuan, N., T. S. Yeo, X. C. Nie, and L. W. Li, "RCS computation of composite conducting-dielectric objects with junctions using the hybrid volume-surface integral equation," *Journal of Electromagnetic Waves and Applications*, Vol. 19, No. 1, 19–36, 2005.
4. Mallahzadeh, A. R., M. Soleimani, and J. Rashed-Mohassel, "RCS computation of alrplane using parabolic equation," *Progress In Electromagnetics Research*, PIER 57, 265–276, 2006.
5. Valle, L., F. Rivas, and M. F. Catedra, "Combining the moment method with geometrical modelling by NURBS surfaces and Bezier patches," *IEEE Trans. on AP.*, Vol. 42, No. 3, 373–381, 1994.
6. Chen, M., X. W. Zhao, Y. Zhang, and C. H. Liang, "Analysis of antenna around nurbs surface with iterative MOM-PO technique," *Journal of Electromagnetic Waves and Applications*, Vol. 20, No. 12, 1667–1680, 2006.
7. Perez, J. and M. F. Catedra, "Application of physical optics to the RCS computation of bodies modeled with NURBS surfaces," *IEEE Trans. on AP.*, Vol. 42, No. 10, 1404–1411, 1994.
8. Chen, M., Y. Zhang, and C. H. Liang, "Calculation of the field distribution near electrically large nurbs surfaces with physical-optics method," *Journal of Electromagnetic Waves and Applications*, Vol. 19, No. 11, 1511–1524, 2005.
9. De Adana, F. S., I. G. Diego, O. G. Blanco, P. Lozano, and M. F. Catedra, "Method based on physical optics for the computation of the radar cross section including diffraction and double effects of metallic and absorbing bodies modeled with parametric surfaces," *IEEE Trans. on AP.*, Vol. 52, No. 12, 3295–3303, 2004.
10. Domingo, M., F. Rivas, J. Perez, R. P. Torres, and M. F. Caredra, "Computation of the RCS of complex bodies modeled using NURBS surfaces," *IEEE Antennas and Propagation Magazine*, Vol. 37, No. 6, 36–47, 1995.
11. Youssef, N. N., "Radar cross section of complex targets," *Proc. IEEE*, Vol. 77, No. 5, 722–734, 1989.
12. Wang, M., M. Chen, and C. H. Liang, "Ludwig algorithm's improvement and its application on NURBS-PO method," *IEEE International Symposium on Microwave, Antenna, Propagation and EMC Technologies for Wireless Communications Proceedings*, 2005.
13. Shi, F.-Z., *CAGD & NURBS*, China Higher Education Press, 2001 (in Chinese).

14. Ruan, Y.-Z., *Radar Cross Section and Sealth Technology*, National Defence Industry Press, Beijing, 1998 (in Chinese).
15. Xue, M.-H. and Z.-R. Wang, "The comprehensive evaluation on the electromagnetic scattering of F16," *Aerospace Electronic Warfare*, Vol. 2, 7–10, 1999 (in Chinese).